Clays and Clay Minerals, Vol. 42, No. 2, 114–122, 1994.

DIOCTAHEDRAL TOSUDITE IN HYDROTHERMALLY ALTERED PLIOCENE RHYOLITIC TUFF, NEUTLA, MEXICO

Liberto de Pablo-Galan[1] and M. L. Chávez-García[2]

[1] Instituto de Geología, Universidad Nacional Autonoma de México, Ciudad Universitaria, 04510 México, D.F.

[2] Facultad de Química, Universidad Nacional A. de México, Ciudad Universitaria, 04510 México, D.F.

Abstract—Dioctahedral tosudite, a regular interstratification of dioctahedral chlorite-dioctahedral smectite, occurs associated with kaolin in the hydrothermal area of Delgado, Neutla, Mexico. Its composition corresponds to the formula:

$$(Si_{13.77}Al_{2.23})Al_8O_{40}(OH)_8 \cdot Ca_{0.39}Na_{0.03}K_{1.06} \cdot (Al_{3.79}Fe^{+3}_{0.09}Fe^{+2}_{0.06}Mg_{0.26})(OH)_{12}.$$

It forms as thin irregular flakes up to 5 μm in size. Adsorbed and cation hydration interlayer H_2O is lost at 81°C and 184°C, dehydroxylation is intense at 496°C and weak at 656°C, with recrystallization at 970°C and 989°C. Infrared analysis shows OH-stretching at 3605 cm^{-1} assigned to the Al–OH–Al group and at 3628, 3500, and 3365 cm^{-1}. Also, OH-bending occurs at 822 cm^{-1}, deformation of the H_2O molecule at 1630 cm^{-1}, Si–O stretching at 1020 cm^{-1}, and bending at 482 cm^{-1}, displaced by Al substitution and increase of the Si–O distance. The characteristic basal spacing of 29.49 Å for the air-dry mineral is changed to 31.32 Å when solvated and to 23.23 Å upon heating; d_{060} = 1.496 Å. The interstratification is a regular 1:1 dioctahedral chlorite-dioctahedral smectite, R = 1, with coefficient of variability 0.73% for the air-dried mineral and 0.76% for the solvated one.

Key Words—Chlorite-smectite clay; Clays; Di,tosudite; Mexico; Mixed-layer clay; Tosudite.

INTRODUCTION

Chlorites form mixed-layer minerals with smectites and other phyllosilicates in which the interstratified layers are di- or trioctahedral, in variable proportions (Bailey, 1988; Reynolds, 1988). Minerals described with trioctahedral or di,trioctahedral layers include tosudite, a regular interstratification of di,trioctahedral chlorite-montmorillonite (Sudo and Kodama, 1957; Shimoda, 1975); a di,trioctahedral chlorite-montmorillonite associated with iron ores in Michigan (Bailey and Tyler, 1960); sudoite from Ottre, Belgium, with a dioctahedral 2:1 layer plus a trioctahedral interlayer (Bailey and Brown, 1962; Eggleton and Bailey, 1967; Fransolet and Bourguignon, 1975; Cheng-Yi and Bailey, 1985); sudoite in the Visean K-bentonites from Anhée, Belgium (Anceau, 1992); Li-cookeite (Bailey and Brown, 1962); and donbassite (Drits and Lazarenko, 1967). Less common are those containing only dioctahedral layers, among which the best known mineral is di,dioctahedral tosudite (Sudo *et al.*, 1954; Sudo and Hayashi, 1956; Sudo and Kodama, 1957; Frank-Kamenetsky *et al.*, 1965; Shimoda, 1969; Imai and Watanabe, 1972; Furbish, 1975); and those containing Li in the gibbsitic interlayer (Nishiyama *et al.*, 1975). Tosudite, or corrensite, as it has been called, has been reported to occur in hydrothermal areas; sedimentary environments in Nigeria (Pacquet, 1968); Permian red beds of the Lisbon Valley, Utah (Morrison and Parry, 1986); the Wellington Formation of Lyons, Kansas (Kopp and Falls, 1974); clastic sediments; and soils (Kübler, 1973). It is uncommon, usually found in small amounts associated with other clay minerals in only a few localities (Bettison and Schiffman, 1988; Brusewitz, 1986). The names tosudite and corrensite (Kopp and Falls, 1974; Morrison and Parry, 1986; Brigatti and Poppi, 1984) have often been used interchangeably in the literature.

The present paper will describe the mineralogy and composition and speculate on the origin of a Li-free regular interstratified mineral formed by dioctahedral smectite and dioctahedral chlorite layers, adding new data on the mineral and a new locality. The tosudite discussed here comes from the hydrothermal zone of Delgado, Neutla, located in the state of Guanajuato, Mexico, between 20°44′ and 20°42′N latitude and 100°52′ and 100°55′W longitude, extending over an area of 10 sq km. Neutla can be reached easily by the Celaya-San Miguel Allende Highway.

GEOLOGY

The geology of the area, based on the work of Reyes-Serna *et al.* (1959), Ledezma-Guerrero (1960), and Comisión de Estudios del Territorio Nacional (1973), is shown in Figure 1. The oldest rocks exposed are intermediate intrusives of Mesozoic age emplaced in Mesozoic marine sediments folded during the Laramide Orogeny of the Cretaceous and Tertiary. The Middle Tertiary is characterized by rhyolitic lava, breccia, and tuff of the Neutla Volcanic Group. New explosive rhyolitic vulcanism in the Lower Pliocene filled the basins with pyroclastics (La Nopalera Formation), which were later altered to bentonite, and continued

Copyright © 1994, The Clay Minerals Society

https://doi.org/10.1346/CCMN.1994.0420202 Published online by Cambridge University Press

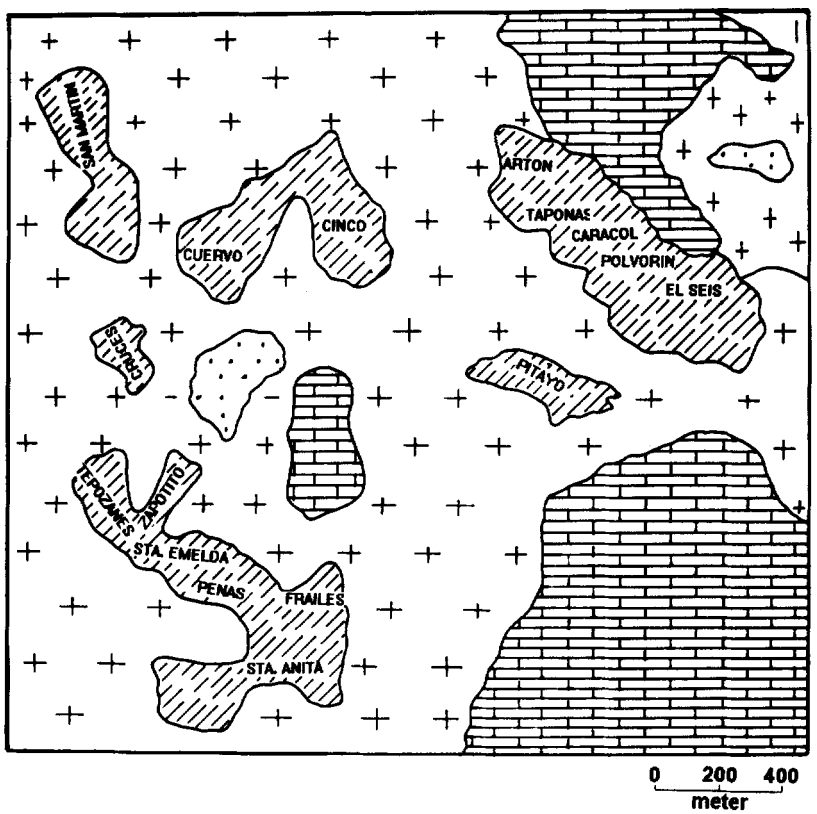

Figure 1. Location of the area between 100°52′–100°55′ and 20°42′–20°44′, NW of Neutla, in the state of Guanajuato, Mexico, indicating the most important clay deposits. The main outcrops of tosudite are in the mines of El Seis, Polvorin, and El Cuervo. Based on data taken from Comision de Estudios del Territorio Nacional (1973) and Consejo de Recursos Minerales (1982).

through the Middle Pliocene with the deposition of volcanic ash and rhyolite up to 80 m thick. The tuff, containing large fragments of pumice and rhyolite in a matrix of glass with quartz phenocrysts, was transformed to clay. Towards the end of the Pliocene, alluvial material accumulated and basalt and andesitic tuff were deposited during the Quaternary.

Hydrothermal alteration of the rhyolites through volcanic chimneys resulted in extensive kaolinization (Figure 1). The kaolin is white, with well-crystallized kaolinite associated with primary and secondary quartz, opal, chalcedony, alunite, and glass. In some deposits, the upper 3 m just under a thin layer of top soil are reddish brown. The composition of the kaolin is not uniform and can rapidly change from highly pure kaolinite in veins about 3 m wide along the fissures through which the vapors ascended to silicic or alunitic kaolins high in opal, chalcedony, alunite, and glass away from the fissures. Some patches of green chlorite are found in the kaolin. To the east of the field, in the El Seis mine (Figure 1), this kaolin is underlain by a very pure plastic kaolin of fine particle size which is mined in tunnels about 6 m wide following the alteration. On the west side of the field, at the El Cuervo mine, the

https://doi.org/10.1346/CCMN.1994.0420202 Published online by Cambridge University Press

kaolin is in contact with bentonite. There is a white to light green plastic clay, locally referred to as plastic kaolin, corresponding to the tosudite presently studied that forms nodules or small lenses in the kaolin and in the bentonite. It is locally known as Seis Primera Verde and Seis Plastico. The most notable outcrop is in the El Seis mine, extending over an area 500 m in the NW-SE direction by 300 m in the NE-SW direction. On the NE side of the field, it is also found in the El Polvorin and El Cuervo mines (Figure 1).

METHODS

The samples collected at the El Seis and El Cuervo mines (Figure 1) were essentially monomineralic as seen with the simple binocular microscope or by X-ray diffraction. Sample purification did not require more than light crushing, ultrasonic dispersion in distilled water without using any chemicals, sedimentation of the coarse material from the fine dispersed clay, and drying at 60°C prior to analysis.

Optical microscopy utilizing oil immersion methods was used to identify the non-clay minerals in the bulk material. The authigenic minerals, bulk and purified, were identified by X-ray diffraction (XRD) of randomly oriented and of sedimented air-dry and ethylene glycol solvated samples using a Siemens D5000 diffractometer (filtered CuKα radiation) with digital readout of the 2θ angle and the peak intensity. The clays were solvated by adding ethylene glycol directly to an aqueous suspension. The thermal behavior of the clay was characterized by differential thermal analysis (DTA) at a heating rate of 10°C/min combined with heating experiments at selected temperatures and XRD of the heated materials. Infrared absorption spectrometry (IR) was applied using a Perkin-Elmer 783 double beam spectrometer operated at a scanning speed of 1000 cm^{-1}/min from 4000 cm^{-1} to 2000 and at 500 cm^{-1}/min between 2000 cm^{-1} and 200 wavenumbers, on the purified mineral dried at 100°C and pressed into KBr discs.

Chemical analyses were performed on the purified clay (dried at 100°C) using X-ray fluorescence (XRF) for the major components and wet chemistry for Na, Fe^{+3}, and Fe^{+2}. H_2O^- represents the water removed at 100°C, which averaged 5.59%; a minor amount of additional H_2O, about 1%, was separated by heating to 200°C. H_2O^+ was measured as the ignition loss at 800°C on material previously dried at 100°C. To calculate the structural formula of the mineral, the mixed-layer chlorite/smectite model was used (Reynolds, 1988): 1), assuming that both 2:1 layers of chlorite and smectite had the same composition; 2), positive charges were balanced on the basis of 100 negative charges ($O_{40}(OH)_8(OH)_{12}$); 3), Si was assigned to tetrahedral positions, adding the Al required to bring the total cation content to 16; 4), octahedral Al was assigned to 8, with the site occupancy on the octahedral sheet of the 2:1 layers assumed to be the same; 5), remaining Al and residual cations were allocated to the chlorite interlayer; and 6), Ca, Na, and K were assumed to be in interlamellar exchangeable positions. Microtextural relations, crystallization, and morphology were interpreted on gold-covered fractured surfaces using a Jeol scanning electron microscope (SEM). Chemical analyses in the SEM were performed by means of a Kevex energy dispersive X-ray spectrometer (EDS) on carbon covered, flat, unpolished, essentially monomineralic specimens. Due to the errors inherent in the technique, these analyses should only be considered as semiquantitative.

Simulated diffraction patterns were computed using the model of MacEwan *et al.* (1961) and the program of Vila and Ruiz-Amil (1988) and compared with the patterns recorded for the oriented clays. The calculation required the use of the atomic distributions and concentrations calculated in the structural formula and the atomic positions known for the chlorite and smectite layers, considering the chlorite cell as extending from the Al-octahedral plane in one layer to the same plane in the next layer and including the octahedral interlayer; whereas, the smectite layer included the exchangeable cations. The type of interstratification (Eggleton and Bailey, 1967; Reynolds, 1988; Bailey, 1988) was identified from the interplanar spacing of the basal reflections recorded for the sedimented unsolvated and solvated clay. The simulated diffraction patterns were calculated, assuming that the square of the layer structure factor was the sum of the squared factors of the chlorite and the smectite layers times their frequencies for several possible layer associations, mixing functions, and angular factors. A thermal coefficient of zero was applied throughout the calculation.

RESULTS AND DISCUSSION

Tosudite from Delgado, Neutla, is white to light green, conchoidal, plastic, soft, and of fine particle size. Megascopically, it resembles bentonite. It is a very pure and uniform clay with only minor quartz, opal, and glass identified microscopically. By XRD, it is essentially monomineralic with very minor segregated illite and, by SEM, some crystals of kaolinite detected in one specimen. No other authigenic mineral was observed.

Chemical composition

The chemical composition averaged from the purified samples (Table 1) corresponds to the structural formula:

$$(Si_{13.77}Al_{2.23})Al_8O_{40}(OH)_8 \cdot Ca_{0.39}Na_{0.03}K_{1.06} \cdot (Al_{3.79}Fe^{+3}_{0.09}Fe^{+2}_{0.06}Mg_{0.26})(OH)_{12}$$

The contents of Fe and Mg are less than Li-tosudite (Nishiyama *et al.*, 1975) and are lower in Si, Al, and Mg and higher in Ca and K than the Li-free tosudite

https://doi.org/10.1346/CCMN.1994.0420202 Published online by Cambridge University Press

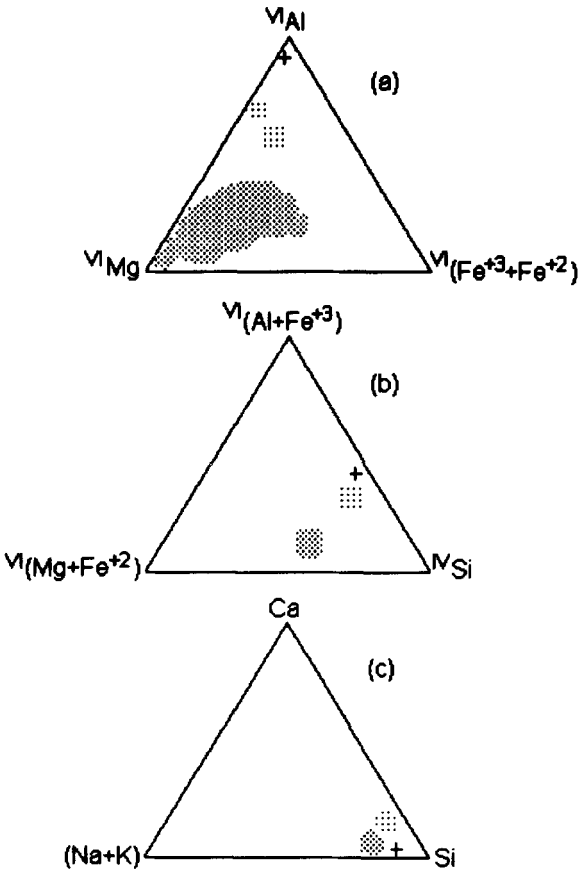

Figure 2. Compositional relations in tosudite from Neutla: a), in the gibbsitic interlayer; b), tetrahedral *vs.* octahedral cations; and c), Si *vs.* exchangeable cations. Dashed areas represent compositions of interstratified chlorite/smectite and Al-chlorite/montmorillonite taken from Brigatti and Poppi (1984).

from Takatama (Shimoda, 1969) and Huy (Brown *et al.*, 1975). With respect to the corrensite from Lisbon Valley (Morrison and Parry, 1986), it shows higher contents of Al and lower of Mg. Tetrahedral Al at 2.23 atoms and the octahedral interlayer cations at 4.20 atoms per formula unit are, respectively, above the ranges of 0.6–1.3 Al atoms per formula unit and within the limits of 4.2–4.5 atoms reported for dioctahedral donbassite (Bailey and Lister, 1989; Anceau, 1992). Octahedral Mg is less than the lower limit of 1.2 atoms per formula unit given for di,trioctahedral sudoite (Anceau, 1992). When plotted in a ^{VI}Mg–^{VI}Al–^{VI}Fe diagram, it is located close to the Al corner, far from other corrensites (Brigatti and Poppi, 1984), confirming the dioctahedral character of the chlorite interlayer. In the $^{VI}(Mg + Fe^{+2})$–$^{VI}(Al + Fe^{+3})$–^{IV}Si system, the composition falls midway close to the $(Al + Fe^{+3})$–Si axes, with the Al higher than other interstratified Al-chlorite/montmorillonites and much higher than trioctahedral mixed-layers, and in the (Na + K)–Ca–Si system falls close to the Si corner, as other reported corrensites (Figure 2).

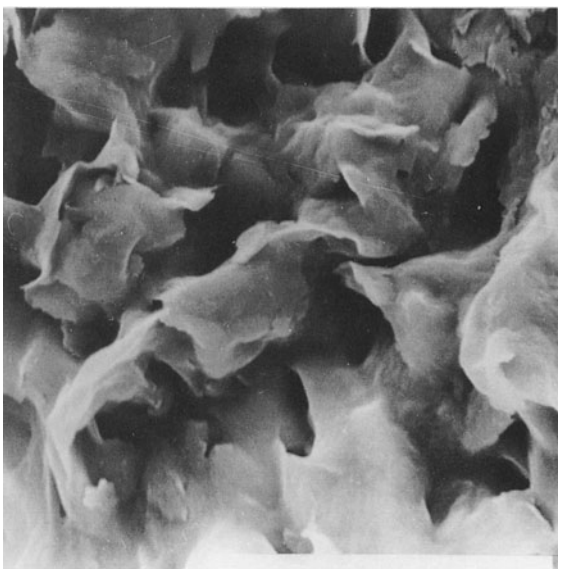

Figure 3. Scanning electron micrograph of tosudite showing crystallization of irregular flakes. 3000×, and the horizontal bar represents 1 μm.

Scanning electron microscopy

Tosudite from Neutla has the morphology of thin irregular flakes (Figure 3), considered typical of smectite mixed-layer minerals (Pollastro, 1985). EDS analyses of selected crystals in flat unpolished specimens revealed 51.02% SiO_2, 44.45% Al_2O_3, 0.68% Fe_2O_3, 0.10% MgO, 0.97% CaO, and 1.83% K_2O which, when combined with the 13.52% H_2O^+ determined by ignition, corresponds to the formula:

$$(Si_{13.89}Al_{2.11})Al_8O_{40}(OH)_8 \cdot Ca_{0.28}K_{0.63} \cdot (Al_{4.13}Fe_{0.14}Mg_{0.04})(OH)_{12}.$$

This formula is comparable, with only less K, to that determined from the more accurate chemical analyses on the purified sedimented mineral (Table 1). It confirms the dioctahedral nature of the mineral and, from the difference between the chemically analyzed K and that recorded by EDS, the association of minor segregated illite.

Differential thermal analysis

Adsorbed water and cation hydration water are lost at 81°C and 183°C, respectively (Figure 4), which are lower than the temperatures of 126°C and 207°C reported for the same reactions for Li-bearing tosudite (Nishiyama *et al.*, 1975). The weak intensity of these endothermic peaks suggests that only minor quantities of water were retained by the purified clay after drying at 100°C. The intense dehydroxylation starting at 370°C and reaching a maximum at 496°C is attributed to

https://doi.org/10.1346/CCMN.1994.0420202 Published online by Cambridge University Press

Table 1. Chemical composition of dioctahedral corrensite from Neutla.

	Composition (wt %)[1]
SiO_2	43.51
TiO_2	0.02
Al_2O_3	37.66
Fe_2O_3	0.37
FeO	0.23
MgO	0.55
MnO	0.05
CaO	1.15
Na_2O	0.05
K_2O	2.63
H_2O^+	13.52
Total	99.74
^{IV}Si	13.774
^{IV}Al	2.226
^{VI}Al	11.795
Fe^{+3}	0.088
Fe^{+2}	0.061
Mg	0.259
Mn	0.013
Ca	0.390
Na	0.031
K	1.061
HO^-	20.000
$O^=$	40.000

[1] Analysis by XRF and wet chemistry.

dehydroxylation of the gibbsitic interlayer. This is not far below the 527°C at which the chlorite interlayer collapses in Li-bearing tosudite (Nishiyama *et al.*, 1975). This temperature of 496°C, which is more in the range reported for the dehydroxylation of palygorskites (Grim, 1962), is higher than the temperature normally assigned to the dehydroxylation of gibbsite (below 300°C) and lower than expected for the dehydroxylation of the chlorite and smectite octahedral layers. The large size of the reaction peak plus the weak dehydroxylation recorded at 656°C suggests that the reaction might include hydroxyls from the interlayer and from the silicate octahedral layers. High-temperature phases crystallize at 970°C and 989°C, higher than the temperatures of 930° and 955°C typical of Li-tosudite (Nishiyama *et*

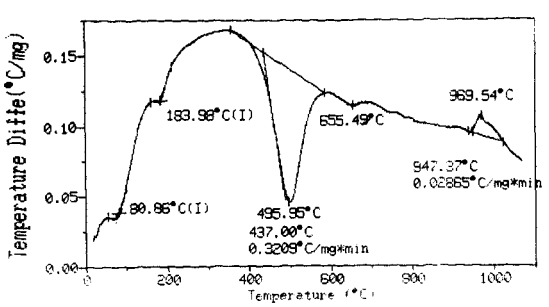

Figure 4. Differential thermal analysis of the dioctahedral tosudite from Neutla.

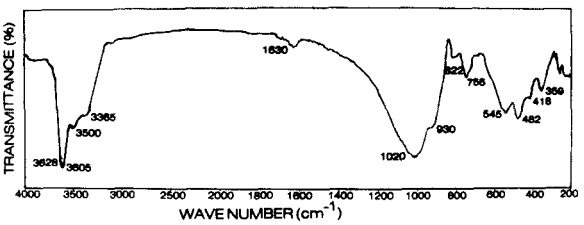

Figure 5. Infrared absorption spectrum of air-dried dioctahedral tosudite.

al., 1975)—most probably because of the higher content of Al in the mineral from Neutla.

Infrared absorption spectrometry

Tosudite is characterized by an intense OH-stretching absorption band at 3605 cm^{-1} (Figure 5), which corresponds to the predominant inner octahedral group Al–OH–Al of the 2:1 layer (Shirozu, 1980). The shoulder at 3628 cm^{-1}, also attributed to inner OH in chlorites (Shirozu, 1980), can suggest additional Al–OH–Mg, Mg–OH–Mg, or Al–OH–Fe octahedral associations. They are displaced with respect to the frequencies of 3685 and 3570 cm^{-1} reported for trioctahedral mixed-layer chlorite-smectite (Bergaya *et al.*, 1985). The displacement, particularly between the 3628 and 3685 cm^{-1} vibrations, may be attributed to the more dioctahedral character of this tosudite or to the effect of higher Al content on the repulsion between atoms (Povarennykh, 1978). OH-stretching from the gibbsitic interlayer—where Al shares positions with Fe^{+3}—and with Fe^{+2}, Mg, and Mn, which would decrease repulsion and increase the frequency of vibration, could be represented by peaks at 3500 cm^{-1} and 3365 cm^{-1}, displaced from the 3427 cm^{-1} signal reported for brucitic interlayers (Serratosa and Viñas, 1964; Hayashi and Oinuma, 1967), or by the 3560 and 3420 cm^{-1} bands ascribed to interlayer OH or (SiSi)O–OH and (SiAl)O–OH vibrations in chlorites (Shirozu, 1980). The vibrations at 3628 and 3365 cm^{-1} confirm the dioctahedral nature of this tosudite compared with those vibrations at 3685 and 3427 cm^{-1} published for trioctahedral mixed-layer minerals. Vibrations at 822 cm^{-1} and 755 cm^{-1} are associated with interlayer OH-bending from Al–OH–Al bonds; they are not far from the 670–650 cm^{-1} usually assigned to trioctahedral Mg–OH–Mg groups (Farmer, 1974) or from the bands at 800 and 720 cm^{-1} assigned to (SiSi)O–OH and (SiAl)O–OH, respectively (Shirozu and Ishida, 1982). A flat region between 680 and 720 cm^{-1} could represent a weak signal coincident with the 692 cm^{-1} band (Hayashi and Oinuma, 1967; Stubican and Roy, 1961) attached to Si–O. The weak band at 1630 cm^{-1}, also reported for Li-tosudite (Nishiyama *et al.*, 1975), is assigned to the deformation of the H_2O molecules adsorbed in the interlamellar spacing. Other vibrations recorded are Si–O stretching and bending at 1020 cm^{-1}

https://doi.org/10.1346/CCMN.1994.0420202 Published online by Cambridge University Press

Table 2. X-ray powder diffraction data of dioctahedral tosudite from Neutla.

	Non-oriented				Sedimented					
	Air-dry		Heated 600°C		Air-dry			Solvated		
hkl	d(A)	I	d(A)	I	d(A)	I	dxorder	d(A)	I	dxorder[1]
001	29.6	14	23.2	10	29.6	57	29.6	31.5	97	31.5
002	14.8	14	11.4	12	14.8	100	29.6	15.7	100	31.5
003	9.81	10			9.81	16	29.4	10.27	31	30.8
004	7.32	15	5.01	13	7.30	7	29.2	7.89	20	31.5
005	5.93	16			4.85	13	29.1	5.22	50	31.3
006	4.85	13	3.76	18	4.85	13	29.1	5.22	50	31.3
007			3.321	30				4.48	94	31.4
020	4.45	100	4.469	100						
021	4.28	44								
022	4.09	34								
008	3.70	23	3.030	18	3.70	16	29.6			
023	3.520	41	3.321	30						
009	3.282	25	2.578	28	3.282	27	29.5	3.490	67	31.4
0010	2.923	23	2.400	10	2.923	14	29.2	3.113	39	31.1
0011	2.698	14	2.240	13	2.698	4	29.6	2.848	28	31.1
0012			2.000	7						
201	2.560	68	2.400	8						
202	2.505	45								
203	2.374	26								
040	2.240		2.240	13						
	2.000	7								
	1.750	6								
242	1.668		1.680	7						
	1.640	8								
	1.518	10								
060	1.496	48								
Mean							29.4			31.3
Sum							0.4			0.2
Std. dev.							0.2			0.2
CV (%)							0.736			0.761

[1] dxorder is the product of the spacing times the order of the reflection.

and 482 cm^{-1} shifted from those at 1005 cm^{-1} and 440 cm^{-1} reported for trioctahedral corrensite (Tuddenham and Lyon, 1959), which indicate higher tetrahedral Si/Al substitution in dioctahedral tosudite. The higher wavenumbers recorded for this tosudite would suggest that it is less ordered than its trioctahedral counterparts (Fripiat *et al.*, 1965; Bergaya *et al.*, 1985).

X-ray diffraction

The XRD data (Table 2) confirm that the mineral is dioctahedral, d_{060} = 1.496 Å, without any trioctahedral component as per the criteria accepted to define chlorite interstratifications (Eggleton and Bailey, 1967; Bailey, 1988; Reynolds, 1988). Diffractograms of air-dried non-oriented, and oriented sedimented aggregates indicated a mean basal spacing of 29.5 Å, which corresponds to one chlorite layer (14.2 Å) plus one smectite layer (15.3 Å). Upon solvation, it expanded to a mean total spacing of 31.3 Å or to 17.1 Å of the smectite layer plus 14.2 Å for the chlorite layer. When heated to 600°C, the spacing decreased to 23.2 Å or to 9.23 Å for the smectite layer plus 14.0 Å for the chlorite. These spacings do not correspond with those of high-charge corrensite (trioctahedral chlorite/Mg-vermiculite) normally characterized by d(001) = 28.5 Å or 14.2 Å spacing of chlorite plus 14.3 Å of the two water Mg-vermiculite layer. The mean d(001) = 31.3 Å measured for the solvated material is closer to that of 31.1 Å reported for low-charge corrensite (trioctahedral) and tosudite (dioctahedral) (Reynolds, 1988); the rationality of the diffraction pattern (Table 2) with I_{002} more intense than I_{001}, $I_{009} > I_{006} > I_{001}$, and reflection 005 absent is more indicative of dioctahedral tosudite (dichlorite/dismectite) than it is of low-charge trioctahedral corrensite typified by $I_{004} > I_{009}$. The spacings also correspond with those of 29.4 Å and 31.6 Å reported for unsolvated and solvated Li-bearing tosudite (Nishiyama *et al.*, 1975), but the ratio of the intensities is different, with the mineral from Neutla having $I_{002} > I_{001}$. Li-tosudite and the tosudite from Neutla have relatively weaker 003 reflections than trioctahedral corrensite and sudoite (Anceau, 1992).

The rationality of the diffraction pattern was tested by calculating the coefficient of variability (CV), which according to the recommendations of the AIPEA Nomenclature Committee (Bailey, 1982) should be less than 0.75% for regular interstratification. Ten orders

https://doi.org/10.1346/CCMN.1994.0420202 Published online by Cambridge University Press

Table 3. Measured and calculated peak diffraction spacings and intensities of dioctahedral tosudite from Neutla.

	Measured		Calcualted[1]				
hkl	d(A)	I	d(A)	F^2	FA	FM	I (%)
001	31.5	97	33.	78,360	2.0	0.093	21
002	15.77	100	15.38	3191	2.0	1.684	16
003	10.27	31	10.52	12,167	2.0	0.456	16
004	7.892	20	8.130	1278	2.0	1.161	4
005			6.290	8577	2.0	1.053	26
006	5.226	50	5.291	13,506	1.9	1.145	44
007	4.487	95	4.525	4727	1.9	1.712	23
008			3.937	7466	1.9	0.515	11
009	3.490	67	3.509	16,278	1.9	2.260	100
0010	3.113	39					
0011	2.848	28	2.865	8150	1.8	2.453	53
0012	2.582	51	2.625	15,537	1.8	0.079	3

[1] F^2, structure factor; FA, angular factor; FM, mixing function.

of reflections were used in the calculation, with odd and even orders having closely similar diffraction widths and without the reflections being streaked towards lower angles. For the air-dried sedimented samples, the mean d_{001} spacing was 29.49 Å, with a standard deviation of 0.21 Å and coefficient of variability equal to 0.73%. For the solvated mineral, the mean basal spacing was 31.32 Å, with a standard deviation of 0.23 Å and a coefficient of variability of 0.76%.

The interstratification between the layers was calculated applying the model of MacEwan *et al.* (1961) and the program of Vila and Ruiz-Amil (1988), using the structural formula calculated and the atomic positions known for the layers (Figure 6). The best fit between the experimental diffraction pattern obtained for the ethylene glycol solvated sedimented clay; and the simulated one (Table 3, Figures 7c and 7d) corresponded to a 1:1 regular interstratification, where R = 1, pA = 0.5, pAA = 0, $d_{chlorite}$ = 14.2 Å, $d_{smectite}$ = 17.2 Å. Comparing the simulated and experimental patterns (Figure 7), the two reflections d(005) = 6.25 Å and d(008) = 3.94 Å, which in the simulated pattern are of medium and low intensity, are not detected in the experimental diffractogram, as has been reported for tosudite (Reynolds, 1988). The reflection recorded at 4.50 Å includes tosudite d(007) and some additional contribution from segregated illite, also represented by the signals recorded at 3.39 Å and 2.57 Å. Otherwise, the simulation fits satisfactorily the experimental pattern (Figure 7) and confirms the classification of the mineral as a regular interstratification of dioctahedral chlorite-dioctahedral smectite, e.g., dioctahedral tosudite.

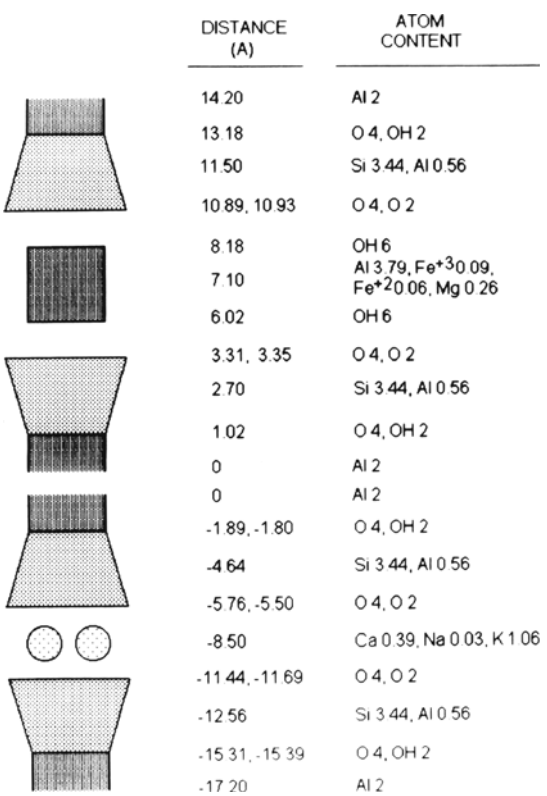

Figure 6. Layer model of tosudite indicating the chlorite and smectite layers used to calculate the diffracted intensities, the simulated diffractogram, and the interstratification, based on structural data from Eggleton and Bailey (1967). The atomic contents correspond with the structural formula computed from the chemical composition of the tosudite from Neutla.

ORIGIN

The evidence presented allows us only to speculate on the origin of tosudite in Neutla, advancing the hypothesis that it could form from precursor volcanics, from smectite, by neoformation, or by a combination of them. Pertaining known transformations have been recognized in the reaction of glass to smectite (Eberl, 1978a, 1978b), of high- to low-charge smectite (Proust *et al.*, 1990), and of low-charge smectite to high-charge smectite+quartz+kaolinite in the formation of illite/smectite and kaolinite/smectite mixed-layers (Meunier *et al.*, 1992). The contents of Al and K and the high Al/Si ratio found in this tosudite, its occurrence, and association with illite, quartz, and opal could suggest diagenesis between precursor smectite and Al- and K-rich fluids to illite, releasing Si and making Al available to form dioctahedral chlorite or to react further with smectite, in a reaction similar to that described for trioctahedral smectites (Środoń, 1980; Środoń *et al.*, 1986; Anceau, 1992). Its tetrahedral Al could originate from dioctahedral smectite, such as beidellite, or from precursor trioctahedral smectite transformed to dioctahedral before reaction. Total Al and the Al/Si ratio are above those expected for smectite/illite systems for which the environment to form mixed-layers has been experimentally found to be within narrow pH limits of 5.5 to 6.5, high pK, and between 100°C and

https://doi.org/10.1346/CCMN.1994.0420202 Published online by Cambridge University Press

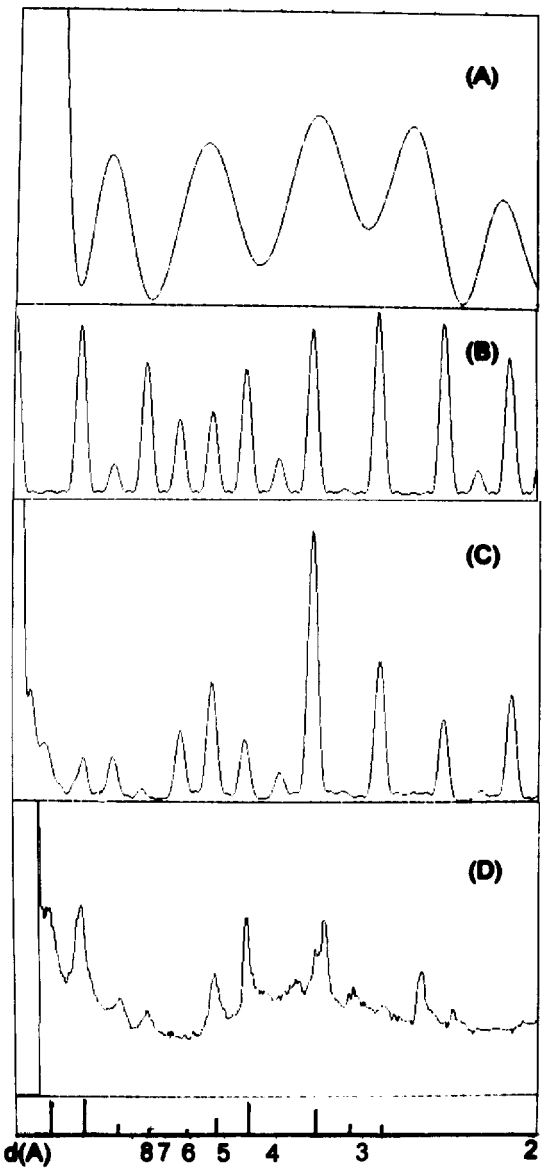

Figure 7. Structural data on the dioctahedral tosudite from Neutla: A), structure factor of the combined chlorite and smectite layers; B), mixing function; C), simulated diffraction pattern; D), experimental diffraction pattern of the ethylene glycol solvated tosudite. Layer frequency is 0.5, probability of one layer following another equal layer is 0, spacing of the chlorite layer is 14.2 Å and of the ethylene glycol solvated smectite layer is 17.2 Å.

150°C that favor tetrahedral coordinated Al (Inoue, 1983; Howard and Roy, 1985; Merino, 1989). High K and K/(Ca + Mg) ratio conform with the observations reported from mixed-layers in bentonites, which required K to balance the layer charge (Velde and Brusewitz, 1982; Brusewitz, 1982). The substantial influx of Al and K needed to form tosudite could result from leaching the underlying shale, the rhyolite tuff, feldspar, or additionally from kaolin. Why smectite/illite was not formed could only be guessed in terms of the abundant concentrations of Al and K, the dioctahedral high-charge character of the 2:1 layers balanced by K, or of particular thermodynamic conditions. Proof of the origin of dioctahedral tosudite in Neutla requires further work and remains to be presented.

ACKNOWLEDGMENTS

The authors are indebted to P. Altuzar, L. Baños, P. Giron, A. Lozano, A. Maturano, G. Pacheco, and M. Reyes for their assistance with the analytical work.

REFERENCES

Anceau, A. (1992) Sudoite in some Visean (Lower Carboniferous) K-bentonites from Belgium: *Clay Miner.* **27,** 283–292.

Bailey, S. W. (1982) Nomenclature for regular interstratifications: *Amer. Mineral.* **67,** 394–398.

Bailey, S. W. (1988) Chlorites: Structure and crystal chemistry: in *Hydrous Phyllosilicates,* S. W. Bailey and P. H. Ribbe, eds., Reviews in Mineralogy, Mineralogical Society of America, Washington, D.C., 347–398.

Bailey, S. W. and Brown, G. E. (1962) Chlorite polytypism: I. Regular and semi-random one-layer structures: *Amer. Mineral.* **47,** 819–850.

Bailey, S. W. and Lister, J. S. (1989) Structures, compositions, and X-ray diffraction identification of dioctahedral chlorites: Clays & Clay Minerals **37,** 193–202.

Bailey, S. W. and Tyler, S. A. (1960) Clay minerals associated with the Lake Superior iron ores: *Econ. Geol.* **55,** 150–175.

Bergaya, F., Brigati, M. F., and Fripiat, J. J. (1985) Contribution of infrared spectroscopy to the study of corrensite: *Clays & Clay Minerals* **33,** 458–462.

Bettison, L. A. and Schiffman, P. (1988) Compositional and structural variations of phyllosilicates from the Point Sal ophiolite, California: *Amer. Mineral.* **73,** 62–76.

Brigatti, M. F. and Poppi, L. (1984) Crystal chemistry of corrensite: A review: *Clays & Clay Minerals* **32,** 391–399.

Brown, G., Bourguignon, P., and Thorez, J. (1975) A lithium-bearing aluminium regular mixed layer montmorillonite-chlorite from Huy, Belgium: *Clay Miner.* **10,** 135–144.

Brusewitz, A. M. (1986) Chemical and physical properties of Paleozoic potassium bentonites from Knneculle, Sweden: *Clays & Clay Minerals* **34,** 442–454.

Cheng-Yi, L. and Bailey, S. W. (1985) Structural data for sudoite: *Clays & Clay Minerals* **33,** 410–414.

Comision de Estudios del Territorio Nacional (1973) Carta Geologica Celaya F-14-C-64, Escala 1:50000: Secretaria de la Presidencia, Mexico, 1 p.

Consejo de Recursos Minerales (1982) Hojas restituidas del area de Delgado, Guanajuato: Consejo de Recursos Minerales, Mexico, 1 p.

Drits, V. A. and Lazarenko, E. K. (1967) The structural and mineralogical character of donbassites: *Mineralog. Sbormik* **21,** 40–48 (in Russian).

Eberl, D. D. (1978a) The reaction of montmorillonite to mixed-layer clays: *Geochim. Cosmochim. Acta* **42,** 1–7.

Eberl, Dennis D. (1978b) Reaction series for dioctahedral smectites: *Clays & Clay Minerals* **26,** 327–340.

Eggleton, R. A. and Bailey, S. W. (1967) Structural aspects of dioctahedral chlorite: *Amer. Mineral.* **52,** 673–689.

https://doi.org/10.1346/CCMN.1994.0420202 Published online by Cambridge University Press

Farmer, V. C. (1974) *The Infrared Spectra of Minerals*: Mineralogical Society, London, 539 pp.

Frank-Kamenetsky, V. A., Logvinenko, N. V., and Drits, V. A. (1965) Tosudite—A new mineral forming the mixed layer phase in alushtite: *Proc. Int. Clay Conf. Stockholm* **II,** 181–186.

Fransolet, A. M. and Bourguignon, P. (1975) Di/trioctahedral chlorite in quartz veins from the Ardenne, Belgium: *Can. Mineral.* **16,** 365–373.

Fripiat, J. J., Rouxhet, P., and Jacobs, H. (1965) Proton delocalization in micas: *Amer. Mineral.* **50,** 1937–1958.

Furbish, W. J. (1975) Corrensite of deuteric origin: *Amer. Mineral.* **60,** 928–930.

Grim, Ralph (1962) *Applied Clay Mineralogy:* McGraw Hill, New York, p. 93.

Hayashi, H. and Oinuma, K. (1967) Si-O absorption band near 1000 cm^{-1} and OH-absorption bands of chlorite: *Amer. Mineral.* **52,** 1206–1210.

Howard, J. J. and Roy, D. M. (1985) Development of layer charge and kinetics of experimental smectite alteration: *Clays & Clay Minerals* **33,** 81–88.

Imai, N. and Watanabe, K. (1972) Tosudite-bearing clay associated with fluorspar deposits of the Igashima mine, Niagata Prefecture, northeastern Japan: *Mining Geol.* **22,** 43–66.

Inoue, A. (1983) K-fixation by clay minerals during hydrothermal treatment: *Clays & Clay Minerals* **31,** 81–91.

Kopp, O. C. and Fallis, S. M. (1974) Corrensite in the Wellington Formation, Lyons, Kansas: *Amer. Mineral.* **59,** 623–624.

Kübler, B. (1973) La corrensite, indicateur possible de millieux de sédimentation et du degré de transformation d'un sédiment: *Bull. Centre Oech. Pau SNAP* **7,** 543–556.

Ledezma-Guerrero, O. (1960) Bosquejo Geologico de la Zona de Neutla, Guanajuato: Tesis, Facultad de Ingenieria, UNAM, 58 pp.

MacEwan, D. M. C., Ruiz-Amil, A., and Brown, G. (1961) Interstratified clay minerals: in *The X-Ray Identification and Crystal Structures of Clay Minerals,* G. Brown, ed., Mineralogical Society, London, 393–445.

Merino, E., Harvey C., and Murray, H. H. (1989) Aqueous chemical control of the tetrahedral aluminum content of quartz, halloysite, and other low-temperature silicates: *Clays & Clay Minerals* **37,** 135–142.

Meunier, A., Proust, D., and Beaufort, D. (1992) Heterogeneous reactions of dioctahedral smectites in illite-smectite and kaolinite-smectite mixed-layers: Application to clay materials for engineered barriers: *Appl. Geochem. Suppl. Issue* **1,** 143–150.

Morrison, S. J. and Parry, W. T. (1986) Dioctahedral corrensite from Permian Red Beds, Lisbon Valley, Utah: *Clays & Clay Minerals* **34,** 613–624.

Nishiyama, T., Shimosa, S., Shimosaka, K., and Kanaoka, S. (1975) Lithium-bearing tosudite: *Clays & Clay Minerals* **23,** 337–342.

Pacquet, A. (1968) Analcime et argiles diagénétiques dans les formations sédimentaires de la région d'Agades (Republic du Niger): *Mem. Serv. Carte Geol. Als.-Lorr.* **27,** 221 pp.

Pollastro, R. M. (1985) Mineralogical and morphological evidence for the formation of illite at the expense of illite/smectite: *Clays & Clay Minerals* **33,** 265–274.

Povarennykh, A. S. (1978) The use of infrared spectra for the determination of minerals: *Amer. Mineral.* **63,** 956–959.

Proust, D., Lechelle, J., Lajudie, A., and Meunier, A. (1990) Hydrothermal reactivity of mixed-layer kaolinite/smectite: experimental transformation of high-charge to low-charge smectite: *Clays & Clay Minerals* **38,** 415–425.

Reyes-Serna, V., Acosta, C., Martinez, J. J., and Nava, J. (1959) Reconocimiento geologico de la zona alunitica de Romero, Guanajuato: *Mineria y Metalurgia* **9,** 93–123.

Reynolds, R. C. (1988) Mixed-layer chlorite minerals: in *Hydrous Phyllosilicates,* S. W. Bailey and P. H. Ribbe, eds., Reviews in Mineralogy, Mineralogical Society of America, 601–629.

Serratosa, J. M. and Viñas, J. M. (1964) Infrared investigation of the OH bands in chlorites: *Nature* **202,** 999.

Shimoda, S. (1969) New data for tosudite: *Clays & Clay Minerals* **17,** 179–184.

Shimoda, S. (1975) X-ray and infrared studies of sudoite and tosudite: *Contributions to Clay Mineralogy in Honor of Prof. Toshio Sudo,* 92–96.

Shirozu, H. (1980) Cation distribution, sheet thickness, and O–OH space in trioctahedral chlorites: An X-ray and infrared study: *Mineral. J.* (Japan) **10,** 14–34.

Shirozu, H. and Ishida, K. (1982) Infrared study of some 7A and 14A layer silicates by deuteration: *Mineral. J.* (Japan) **11,** 161–171.

Środoń, Jan (1980) Synthesis of mixed-layer kaolinite/smectite: *Clays & Clay Minerals* **28,** 419–424.

Środoń, J., Morgan, D. J., Eslinger, E. V., Eberl, D. D., and Karlinger, M. R. (1986) Chemistry of illite/smectite and end-member illite: *Clays & Clay Minerals* **34,** 368–378.

Stubican, V. and Roy, R. (1961) Isomorphous substitution and infrared spectra of the layer lattice silicates: *Amer. Mineral.* **46,** 32–51.

Sudo, T. and Hayashi, H. (1956) Types of mixed-layer minerals from Japan: *Clays & Clay Minerals* **4,** 389–412.

Sudo, T. and Kodama, H. (1957) An aluminous mixed-layer mineral of montmorillonite-chlorite: *Z. Kristallogr.* **109,** 379–387.

Sudo, T., Takahashi, H., and Matsui, H. (1954) Long spacing of 30Å from fireclay: *Nature* **173,** 161.

Tuddenham, W. M. and Lyon, R. J. P. (1959) Relation of infrared spectra and chemical analysis for some chlorites and related minerals. *Anal. Chem.* **31,** 377–380.

Velde, B. and Brusewitz, A. M. (1982) Metasomatic and non-metasomatic low-grade metamorphism of Ordovician meta-bentonites in Sweden: *Geochim. Cosmochim. Acta* **46,** 447–452.

Vila, E. and Ruiz-Amil, A. (1988) Computer program for analyzing interstratified structures by Fourier transform methods: *Powder Diffraction* **3,** 7–11.

(Received 25 February 1993; accepted 9 November 1993; Ms. 2334)

https://doi.org/10.1346/CCMN.1994.0420202 Published online by Cambridge University Press